The electrochemical potential is a key parameter for cell adhesion and proliferation on carbon surface

Simon Guette-Marquet, Régine Basseguy, Christine Roques, Alain Bergel

The electrochemical potential is a key parameter for cell adhesion and proliferation on carbon surface

Simon GUETTE-MARQUET[a], Régine BASSEGUY[b], Christine ROQUES[a], Alain BERGEL[b] *

[a] *Laboratoire de Génie Chimique, Université de Toulouse, CNRS, INPT, UPS, Faculté des Sciences Pharmaceutiques, 35 chemin des maraîchers, 31062 Toulouse cedex 4, France.*

[b] *Laboratoire de Génie Chimique, Université de Toulouse, CNRS, INPT, UPS, 4 allée Emile Monso, 31432 Toulouse, France.*

** Corresponding author: alain.bergel@toulouse-inp.fr*

Abstract

The Nernst potential of the support/cell interface is suspected to play a key role in cell adhesion and proliferation. However, the studies that have addressed this topic have generally varied the electrochemical potential of the interface by comparing different materials or by varying the chemical composition of the surface coating. It is consequently hard to definitively separate the actual effect of the potential from possible side-effects due to differences in the surface composition or topography. Here, a 3-electrode set-up was used to apply different values of potential to identical carbon electrodes. Potentials were applied in the range -200 to 400 mV vs. silver pseudo-reference (SPR), i.e. 90 to 690 mV/SHE, to screen-printed carbon electrodes used to grow Vero or Raw 264.7 cell lines. Values up to 200 mV/SPR prohibited cell adhesion and even caused detachment of cells that were previously adhered. The value of 400 mV/DRP allowed cell adhesion and proliferation, leading to confluent and sometimes very compact mats. The zero charge potential, measured around 200 mV/DRP, showed that the drastic effect of the applied potential was probably due to the negative/positive switch of the surface charge.

Key words: Vero cell; Raw 264.7 cell; Surface charge; Biomaterial; Cell culture; Tissue engineering.

1. Introduction

Animal and human cells are usually cultured on solid supports and the conductivity of the support is a key parameter guiding their development [1–3]. The impact of the support conductivity on cell growth has been demonstrated in many different ways. For instance, the interfacial electrical resistance and the surface charge have been shown to affect the proliferation and differentiation of neural stem cells [4]. The addition of conductive nanoparticles inside a non-conductive support can affect cell proliferation and differentiation [5,6]. It has been reported that the presence of conductive compounds at the surface of the support promote stem cell differentiation towards so-called “electroactive” lineages (neural, cardiac) [7]. Modifying the conductivity of the support is thus thought to open possible paths towards cell growth control [8,9].

In most studies, the impact of the electrochemical status of the interface is approached indirectly by comparing different materials or different coatings [10]. It is consequently difficult to distinguish the possible impact of the electrochemical potential from the effects of other surface properties that may have been modified concomitantly. Actually, many different surface properties have the ability to affect cell adhesion, proliferation and differentiation [11,12]. For example, the chemical composition of the surface [13], its hydrophilic/hydrophobic character [14,15], its topography [16] and the specific adsorption of proteins are well-known impacting factors, and synergetic effects can also occur [17].

Surprisingly, the impact of the Nernst potential on cell growth has rarely been approached directly by applying controlled values of potential to the support. The widespread presence of conductive supports in cell culture and tissue engineering [18–20] has rarely been used to full advantage to grow cells under controlled potential.

In contrast, in the context of microbial cells, growing biofilms under potential is usual and has led to great successes [21]. Microbial biofilms are often formed on electrodes polarized at a given potential value throughout the days, sometimes weeks, required to develop a mature biofilm. This strategy has succeeded in demonstrating the essential role of the Nernst potential on the formation of electroactive microbial biofilms either in multi-species [22,23] or pure culture conditions [24,25]. Surprisingly, similar potential-controlled strategy has not yet been adopted in the context of animal and human cell culture and tissue engineering.

Actually, in the field of cell culture and tissue engineering, many studies have described the growth of cells on polarized electrodes. Unfortunately a great proportion of these studies implemented single-electrode systems [26]. In this case, the current is forced from one edge of the conductive support to the other edge. Theoretical analysis [26] shows that these single-electrode systems create a potential gradient between the edges of the electrode and, consequently, do not allow the potential of the interface to be controlled. Accordingly, in such studies, the potential is rarely measured with respect to a reference electrode.

A group of works has attempted to implement a two-electrode set-up to study cell adhesion and growth [27,28]. Different voltages were applied between the two electrodes. The experimental observations are of interest because the different voltage values were applied to identical electrodes so that the impact of surface parameters other than the electrochemical potential could be excluded. Unfortunately, the potential of the electrodes was neither measured nor known, because no reference electrode was used. A voltage ΔV was applied between the two electrodes and it was postulated that the cathode and the anode had potentials equal to $-\Delta V/2$ and $+\Delta V/2$, respectively. Unfortunately, this assumption is wrong. It was also postulated that the anode had a positive surface charge, because it was connected to the positive pole of the generator, and the cathode a negative surface charge, because it was connected to negative pole. This assumption is also invalid. The sign of the generator poles are related to the direction of electron flow and not to the surface charge of the electrodes.

Three-electrode systems have been largely used to investigate the behaviour of animal and human cells on electrodes. Numerous electroanalytical studies have highlighted the great sensitivity of animal and human cells to the potential of the support. A pioneering work showed that human erythrocytes and leucocytes precipitate on metallic surfaces at a given value of the applied potential [29]. A shift of the potential applied to polypyrrole-coated electrodes can drive membrane rupture and cell lysis of erythrocytes [30]. It has even been claimed that the potential is the only determining factor in the interaction between carbon surface and blood [31]. As reviewed recently [32], the potential of the support can impact cell morphology [33], control cell attachment and detachment, and orient the synthesis of substances [34]. Many inspiring results have also been produced by using cyclic voltammetry (CV). Oxidation peaks were obtained with various cell lines (U937 tumour cells [35], PC-3 [36], HeLa [37], HepG2 cells [38] …), which indicate the presence of redox compounds on the outer membrane. CV peaks were also recorded with human pluripotent cells, depending on their level of differentiation. The peaks were observed with undifferentiated stem cells and vanished with differentiated cells [39].

To sum up, numerous clues and proofs of the sensitivity of cells to the electrochemical potential have been given by analytical studies, i.e. studies performed over a short time with cells in survival conditions, but attempts to grow cells while applying a controlled potential to the support have been rare.

A few studies have started to advance in this direction. They were mainly dedicated to implantable metallic devices and their purpose was to define the range of potentials allowing cell survival on the electrode surface [40–42]. It has thus been stated that, when the applied potential is too low, it drives oxygen reduction, which produces reactive oxygen species (ROS) and imposes oxidative stress on the cells. In contrast, values that are too high induce oxidation of the metallic materials, which releases toxic metallic ions. It was thus possible, depending on the nature of the metal or alloy, to determine a range of potential values in which no detrimental reaction to cell development occurred. However, these studies did not address the effect of the

potential on cell growth within the range where oxygen reduction and metal oxidation do not occur, i.e. in the range where cell culture on the electrode is possible.

To the best of our knowledge, very few examples of cell culture in potential-controlled conditions are reported in the literature. For instance, a human carcinoma line of MKN45 cells cultured on a platinum electrode for 4 days secreted twice as much carcinoembryonic antigen when a potential in the range from 0.2 V to 0.6 V vs. Ag/AgCl was applied, in comparison with the control experiment performed without applied potential [34].

The general objective of the present work is to promote the culture of cells on polarized supports with controlled potential. It seems logical that the first steps in this direction should be taken by studying the effect of the Nernst potential of the electrode/cell interface on cell adhesion and proliferation. Cells were grown on polarized electrodes by using a 3-electrode set-up. The potential was thus controlled with respect to a reference electrode and different values were applied to the same electrode surface. No chemical modification of the surface was necessary to change the potential. It was thus possible to study the effect of the applied potential on cell adhesion and proliferation without changing the chemical composition of the electrode coating.

A commercial, disposable electrochemical set-up composed of small carbon electrodes screen-printed on a ceramic strip was used in order to avoid possible deviation due to homemade electrode systems. Two types of cells were used, the Vero and Raw 264.7 cell lines. The Vero cell line was established from kidney tissue of a green monkey (*Cercopithecus aethiops*) [43] and the Raw 264.7 cell line was composed of macrophage-like cells originating from a mouse (*Mus musculus*) cell line transformed with Abelson leukaemia virus. These two cell lines were chosen here because Vero cells are commonly used in biomedical industries to culture viruses and produce vaccines, and for diagnostic and research purposes [44,45], and Raw cells are a common mouse macrophage model.

Cells were cultured for several days on electrodes polarized at different potentials in the range -200 to +400 mV vs. the silver pseudo-reference (SPR), i.e. +90 to +690 mV vs. the standard hydrogen electrode (SHE). This range was chosen in order to avoid the strong reduction of dissolved oxygen at the lowest values and oxidation of water at the highest.

The potential showed a drastic effect on cell development as neither adhesion nor proliferation was possible at the lowest potential values while, on the contrary, the highest value promoted cell adhesion and proliferation. Determination of the zero charge potential indicated that cell adhesion and proliferation occurred only when the potential drove a positive surface charge. The existence of such a rule has already been speculated in the literature [28] [10], but the present paper is its first experimental demonstration via strict control of the electrode potential, without modifying the chemical composition of the supporting material surface.

These results definitively confirm the great effect of the Nernst potential on cell adhesion and proliferation and explain it by a direct link with the charge surface. The results also demonstrate the great interest of a 3-electrode system to offer a well-controlled polarized surface for cell

growth. As the electrochemical potential of the surface is a crucial parameter, not only in adhesion and proliferation, but also in differentiation and cell signalling [12], this strategy should now be implemented much more systematically to open up new avenues in cell culture, biomaterial design and tissue engineering.

2. Materials and Methods

2.1 Electrodes and electrochemical reactors

Carbon screen-printed carbon electrodes were purchased from Metrohm-DropSens. They were disposable 3-electrode systems, screen-printed on a ceramic strip (Schematic 1). The working and auxiliary electrodes were made of the same carbon material (ref. DRP-110). The working electrode was a disk 4 mm in diameter.

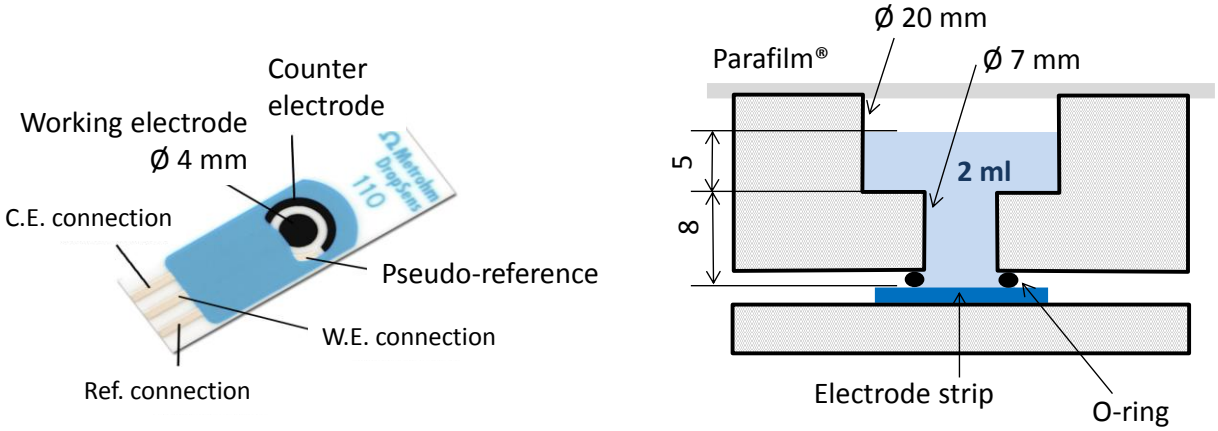

A. Electrode strip **B. Electrochemical reactor**

Schematic 1. *Electrochemical set-up. A) electrode strip, B) electrochemical reactor. The disposable electrode, purchased from DropSens-Metrohm, is a ceramic strip 34 mm long and 10 mm wide, on which the electrodes are screen-printed. The electrode strip was inserted at the base of the electrochemical reactor.*

The reference electrode was a silver pseudo-reference (SPR). In the experimental conditions used in the present study, i.e. after pre-treatment of the electrodes and using the RPMI medium for the measurements, the potential of the DropSens SPR was equal to 0.049 V vs. saturated calomel electrode, i.e. 0.290 V vs. standard hydrogen electrode (SHE). All the potentials are expressed with respect to the silver pseudo-reference (SPR) in this study, which means that it is sufficient to add 49 mV to find the values of potential with respect to the saturated calomel electrode or to add 290 mV to find the values with respect to the standard hydrogen electrode.

All experiments were performed in lab-made electrochemical reactors made of polytetrafluoroethylene and specifically designed for the DropSens electrode strips (Schematic

1). The internal diameter of the reactors was 0.7 cm for the lower part and 2 cm for the upper part. Electrodes were at the bottom of the reactor and were covered by 2 mL of medium. Electrodes were connected to the potentiostat with copper wires, tin soldered to the electrode connectors.

2.2. Cell culture

The Vero cell line (CCL-81™ from ATCC) and Raw 264.7 cell line (TIB-71™ from ATCC) were kindly provided by Fonderephar (Toulouse, France). Cells were cultivated in complete growth medium containing RPMI medium (Gibco) supplemented with 10 % heat inactivated foetal bovine serum (FBS, from Gibco), 2 mM of L-glutamine (Gibco) and antibiotics (penicillin 10 U/ml and streptomycin 10 µg/ml, from Gibco), at 37°C in humidified air with 5% CO_2. Cells were routinely subcultured at 80-90% of confluence.

Cells from a 75 cm² flask at 70-90% of confluence were harvested with trypsin-based buffer (Gibco). After centrifugation at 200 g for five minutes, cell pellets were resuspended in complete growth medium at a density of 50 000 cells/ml (Vero cell line) or 7 500 cells/ml (Raw 264.7 cell line).

2.3 Electrochemical reactor seeding

Prior to use, reactors and electrodes were cleaned in RBS 35 (CarlRoth) bath (2%, in water) for 2 hours and rinsed thoroughly under running tap water. Reactors were sterilized by soaking them in 70% ethanol for 30 minutes. Electrodes were rinsed three times with ultra-pure water. Reactors and electrodes were air-dried for at least two hours in a microbiological safety cabinet. After drying, electrodes were mounted in the reactors. For all experiments, the electrodes were pre-treated with foetal bovine serum (FBS) diluted with an equal volume of phosphate buffer solution (FBS/PBS). For this pre-treatment, reactors were filled with FBS/PBS and incubated in a sterile safety cabinet for 16 hours (experiments with Vero cells) or two hours (experiments with Raw 264.7 cells). Actually, shortening the duration of the pre-treatment from 16 to 2 hours did not lead to any change in the cell behaviour with respect to that observed in experiments carried out with Vero cells, not reported here.

After treatment of the electrodes, the FBS/PBS solution was eliminated and replaced by two millilitres of cell suspension, or by sterile complete growth medium, without cells, for the control experiments. Reactors were closed with sterile Parafilm®, transferred into a cell culture incubator and connected to the potentiostat.

2.4 Incubation in electrochemical reactors

All experiments were carried out in a cell culture incubator at 37 °C in humidified air containing 5 % CO_2. When 4 reactors were run in the incubator, 12 electric wires had to be passed through the grommet of the incubator. The wires were wrapped in aluminium foil to form a Faraday cage, electrically connected to the potentiostat ground. The connections between the electrode strip and the electrical wires were tin soldered, because the connections provided by the manufacturer with the strip, for insertion into a female connector, did not withstand several hours of incubation at 37 °C in 100% humidity.

Different potentials, in the range -200 to 400 mV/SPR, were applied to the working electrode with respect to the pseudo-reference electrode, using a VMP-3 potentiostat (Biologic) monitored by the EC Lab software (Biologic). The current produced was recorded every 10 minutes. Depending on the experimental run, four or five reactors were operated in parallel in the same incubator and addressed individually. In the first experimental run, a first incubation phase of 24 hours was performed without applying any potential, then the potential was applied for 48 hours. In the following experimental runs, the potential was applied from the beginning of the incubation.

2.5 Microscopy and image analysis

After electrochemical recording, the reactors were carefully emptied and the medium was replaced by 500 µl of PBS pre-warmed to 37 °C. After elimination of the PBS, the reactors were filled with 500 µl of staining solution (5 µM Syto® and 1 mg/ml propidium iodine in PBS, from Molecular Probes) and incubated at 37 °C for around 20 minutes. After incubation, electrodes were rinsed with PBS and covered with a coverslip in order to prevent desiccation. Images were acquired with an Axiotech epi-fluorescence microscope (Zeiss), with green (41001HQ F C71828) and red (4100HQ PI C71829) fluorescence filters (Zeiss). Images were processed using Zen software (blue edition, release 2.5, Zeiss). Quantification of cell number was performed with ImageJ software (release 1.53, NIH [46] with the “Find Maxima” function and manual adjustment of the noise tolerance. The number of electrodes and images used for cell quantification is indicated in each figure.

2.6 Electrochemical impedance spectroscopy (EIS)

Before the measurement, the electrodes were pre-treated following exactly the same protocol as for the cell cultures and the Mott-Schottky measurements were performed in sterile complete growth medium in order to be made in the same conditions as during cell cultures. Six different electrodes were used and the measurements were performed twice on each. The electrodes were immersed in the sterile complete growth medium for 1 hour before the first measurement and the first and second measurements were separated by 3 hours.

EIS measurements were carried out with a VMP-3 potentiostat (Biologic) monitored by the EC-Lab11.26 set up following the Staircase Potentio Electrochemical Impedance Spectroscopy

(SPEIS) technique. This technique is designed to perform successive impedance measurements (over a whole frequency range) during a potential sweep. The potential was scanned from -200 to 500 mV/SPR in 14 successive steps or from 0 to 500 mV/SPR in 20 successive steps. For each step, the potential was maintained constant for 5 min before starting impedance acquisition. The sinewave amplitude was 15 mV and frequency ranged from 100 kHz to 50 mHz with 10 points per decade in logarithmic spacing (Nd). A 0.10 period (Pw) was maintained before each frequency and 5 measurements were taken per frequency (Na = 5). For each frequency, the EIS data were analysed by displaying a Mott-Schottky plot, i.e. $1/C^2$ versus E, where C is the interfacial capacitance and E is the applied Nernst potential.

Results and discussion

Five experimental runs were performed successively with Vero cells following the same protocol. For each run, 4 electrochemical reactors (Schematic 1) were operated in parallel:

- 2 reactors were seeded with 100 000 Vero cells each (except in one run, which included 3 of these reactors); the reactors were firstly incubated for 24 hours without applied potential, then the potential was applied for 48 hours, i.e. until the end of the 72-hour experiment.
- one reactor, used as a negative control, was not seeded with cells and the potential was applied similarly after 24 hours of incubation,
- one reactor, used as a positive control, was seeded with 100 000 cells but left without applied potential during the entire 72-hour experiment.

The sole parameter varying from one run to another was the value of the applied potential. One run was performed at -200 mV/SPR, one at 0 mV/SPR, one at 200 mV/SPR and two at 400 mV/SPR. The currents recorded during the phases of applied potential are reported in Figure 1.

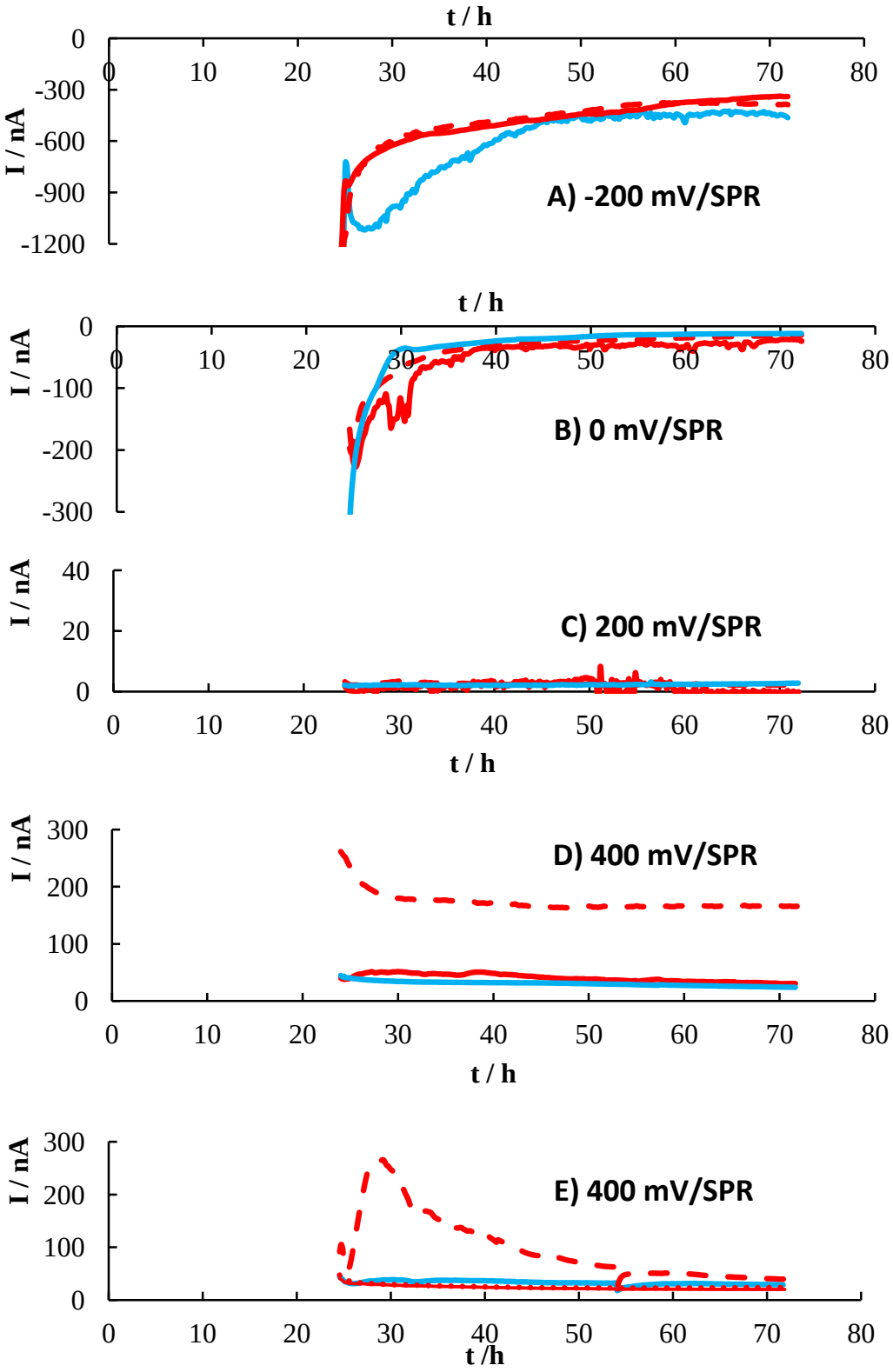

Fig. 1. *Current recorded when the potential was applied for 48 hours after the initial 24-hour incubation without potential. The applied potential was A) -200 mV/SPR, B) 0 mV/SPR, C) 200*

mV/SPR, D and E) 400 mV/SPR. Blue lines: abiotic reactors; red lines: reactors seeded with 100 000 Vero cells.

The applied potential of -200 mV/SPR (Figure 1.A) induced a low reduction current, the intensity of which decreased from around 1100 to 300 nA during the 48 hours of the potential application. This current was due to the slow electrochemical reduction of dissolved oxygen. This has already been shown using the same electrodes in the same medium [47]. The presence of the cells decreased the value of the reduction current because they masked a part of the electrode surface and thus impeded the transport of dissolved oxygen to the electrode surface.

The applied potential of 0 mV/SPR (Figure 1.B) produced a reduction residual current that was less than 50 nA for most of the polarization time. The potential of 200 mV/SPR (Figure 1.C) resulted in a low oxidation residual current, around 2 nA. In both cases, the presence of cells did not modify the current intensities significantly. At 400 mV/SPR (Figures 1.D and 1.E), the abiotic current was stable, at around 30 nA on average, and the presence of the cells tended to increase this oxidation current in some cases, but in a way that was not possible to reproduce well.

At the end of the experiments, the electrodes were extracted from the reactors, gently rinsed, stained and imaged. The electrodes exposed to potentials of -200, 0 and 200 mV/SPR showed no significant colonization (Figure 2). In each of the five runs, one control reactor was left without polarization for the entire 72 hours of the experiment. Four of these electrodes showed a dense mat of adhered cells with an average cell density of 198 150 ± 49 670 cell/cm^2, one displayed a lower surface colonization with an average cell density of 9 270 ± 10 475 cell/cm^2. Comparing the average cell densities obtained after 72 hours without polarization and after 72 hours including 48 hours of polarization clearly showed that the polarization at -200, 0 and 200 mV/SPR severely impeded cell adhesion and growth (Figure 2).

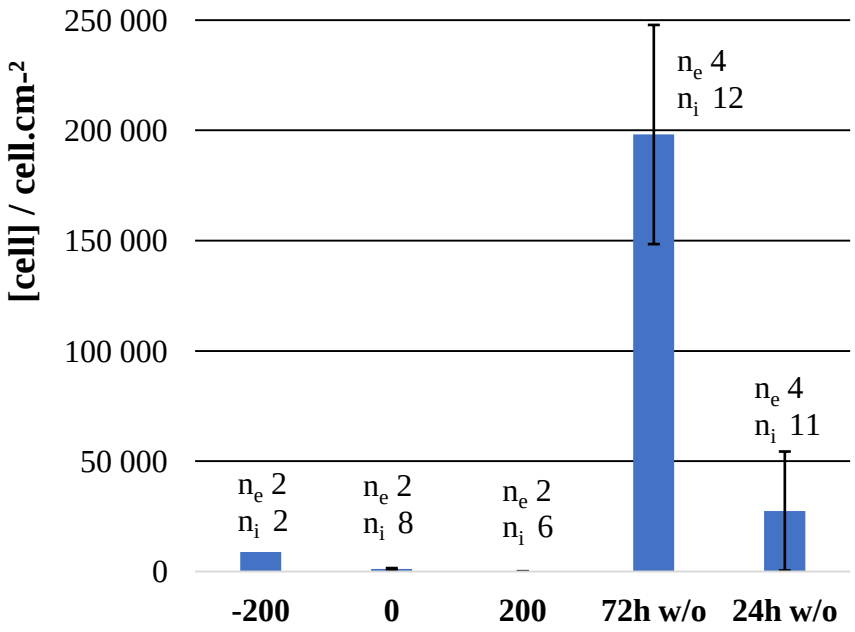

Fig. 2. *Number of adhered Vero cells after 72 hours of incubation. For columns 1 to 3, the potential was applied for 48 hours after the initial 24-hour incubation without potential: potential values of -200, 0 and 200 mV/SPR, respectively; column 4: 72-hour incubation without applied potential; column 5: 24-hour incubation without applied potential; seeding with 100 000 Vero cells.* n_e *is the number of electrodes imaged and* n_i *is the total number of images.*

According to the reactor design schematized in Schematic 1, the solution height above the electrode was around 1.3 cm. The cell density used for seeding was 50 000 cell/ml (100 000 cells in 2 ml). If all the cells contained in the solution above the electrode strip sedimented at the bottom, the cell density at the bottom would be 65 000 cell/cm^2. The average cell density of 198 150 cell/cm^2 found after 72 hours without polarization corresponds to more than one cell generation. This value is consistent with the doubling-time of 24 hours for the Vero line [48].

In contrast to the others, the electrodes exposed to the potential of 400 mV/SPR displayed considerable colonization. Among the 5 electrodes, only one displayed weak colonization (870 ± 400 cell/cm²; n_i = 3, Figure 3.A), while the 4 others showed a very dense cell mat. It was possible to count the adhered cells on only one electrode (Figure 3.B), which gave the value of 99 280 ± 34 300 cell/cm² (n_i = 3). It was not possible to assess cell density for the other 3 electrodes exposed to 400 mV/SPR because they supported a thick, dense cell mat with a structure closer to that of a biofilm than to individual adhered cells (Figure 3.C).

A) 72h including 48h at 400 mV/SPR - Weak colonization

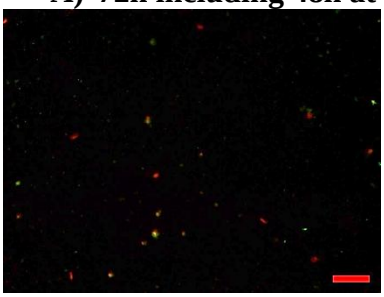

B) 72h including 48h at 400 mV/SPR - Dense mat

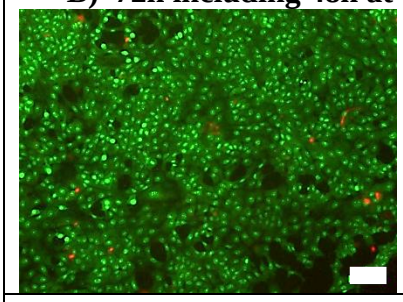

C) 72h including 48h at 400 mV/SPR - Dense mat with biofilm-like structure

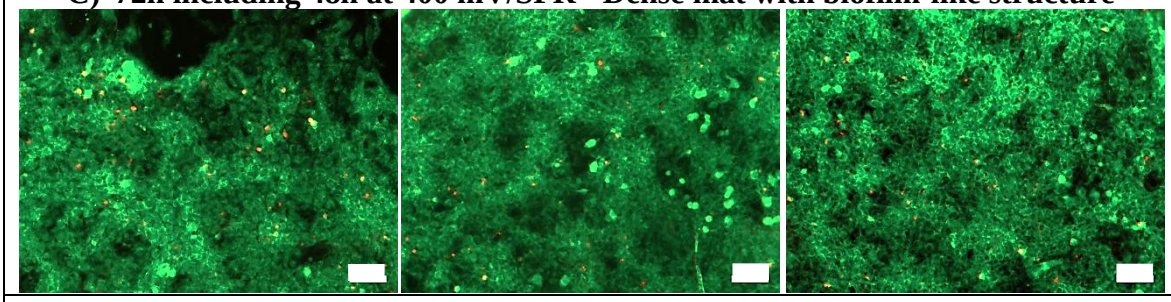

D) 72h without polarization

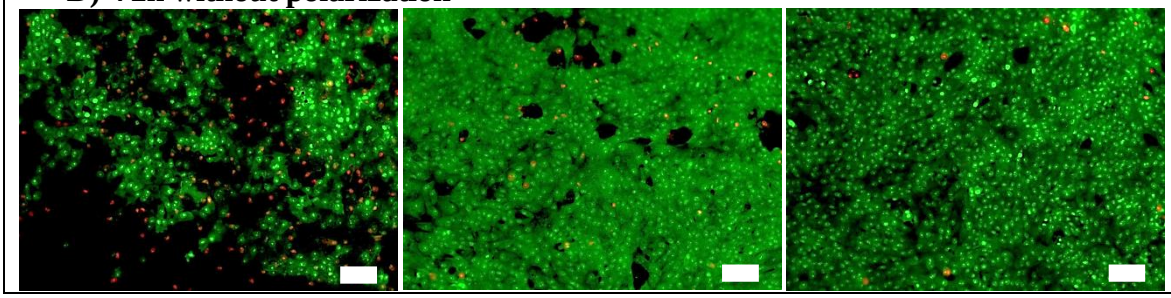

Fig. 3. *Representative pictures of the Vero cell mats after 72 hours' incubation with 48 hours at 400 mV/SPR. A) The electrode with low colonization, B) the electrode with high colonization whose adhered cells could be counted. C) the 3 electrodes that displayed a biofilm-like structure; epifluorescent imaging after staining with Syto® and propidium iodine; scale bar 100 µm.*

When the potential of 400 mV/SPR was applied, the cells adhered to the electrode surface well, resulting in cell mats that were at least as dense as the mats obtained in the absence of

polarization and often denser. There were no cells stained red by the propidium iodide on the images, which proves that the cells were not altered by the 400 mV/SPR potential. All the adhered cells were viable at the end of the 72-hour experiment.

An additional experimental run was carried out with 4 reactors incubated in similar conditions but for only 24 hours and without any applied potential. After 24 hours, the average cell density was 27 500 ± 26 970 cell/cm^2 (Figure 2). The standard deviation was high because the surface colonization was quite inhomogeneous from one image to another. The average measured value of 27 500 cell/cm^2 was lower than the cell density calculated above for simple sedimentation of the cells on the bottom of the reactors (65 000 cell/cm^2, see above). The measured value was smaller, probably because the cells that were not firmly adhered to the surface of the electrodes were washed away during rinsing and staining, although these steps were carried out with great care.

The experiment run without polarization for 24 hours showed that the cells adhered to the electrode surface after the initial 24-hour phase of incubation. Consequently, the applied potentials of -200, 0 and 200 mV/SPR, which were applied after 24 hours of incubation, not only prevented colonization of the electrode surface but also released the cells that had adhered during the initial 24-hour potential-free phase.

Moreover, comparing the cell density after 24 hours of incubation without potential (27 500 ± 26 970 cell/cm^2) and the cell mats obtained after 48 supplementary hours under 400 mV/SPR (Figure 3) showed that the potential of 400 mV/SPR did not impede cell proliferation. The increase from 27 500 cell/cm^2 to 99 280 cell/cm^2, which was measured on one electrode (Figure 3.B), was close to two generations during the 48 hours of polarization. The coverage of the other 3 electrodes exposed to 400 mV/SPR, which displayed a biofilm-like structure (Figure 3.C), was even more dense and suggests that the development may have been promoted by the 400 mV/SPR applied potential.

The polarization at 400 mV/SPR was repeated following the same experimental protocol but, this time, without the initial 24-hour phase when there was no polarization. The potential of 400 mV/SPR was applied immediately after seeding the reactors. Four reactors were run in parallel, one control reactor was not seeded with cells, the other 3 were seeded with 100 000 Vero cells. Among these 3 reactors, one was stopped and the electrode was imaged after 24 hours of polarization, another after 48 hours and the third after 72 hours.

In all cases, the current stabilized quickly during the first hour of polarization and then decreased continuously from about 50 nA initially to 20 nA after 72 hours. The current records displayed no significant difference between the seeded reactors and the abiotic control.

Imaging the electrodes after 24, 48 and 72 hours of polarization at 400 mV/SPR showed a progression in the proliferation of the cells (Figure 4). Only the electrode collected after 24 hours (Figure 4.A) could be analysed in terms of cell density, with a value of 48 515 ± 7 210 cell/cm^2. The electrodes collected after 48 and 72 hours (Figure 4.B and 4.C, respectively) displayed

confluent cell mats, which were too compact and too thick to allow cell densities to be correctly evaluated.

As before, no significant red staining (propidium iodide) was observed. Careful examination could detect a slightly increased number of damaged cells after 72 hours incubation. This remains a very small minority. The increase in dead cells was correlated with the increase in the total number of cells and the progressive depletion of the environment in the absence of renewal. The great majority of cells were viable even after 72 hours of polarization. This run confirmed that the 400 mV/SPR potential was favourable for the adhesion and proliferation of the Vero cells on carbon electrodes.

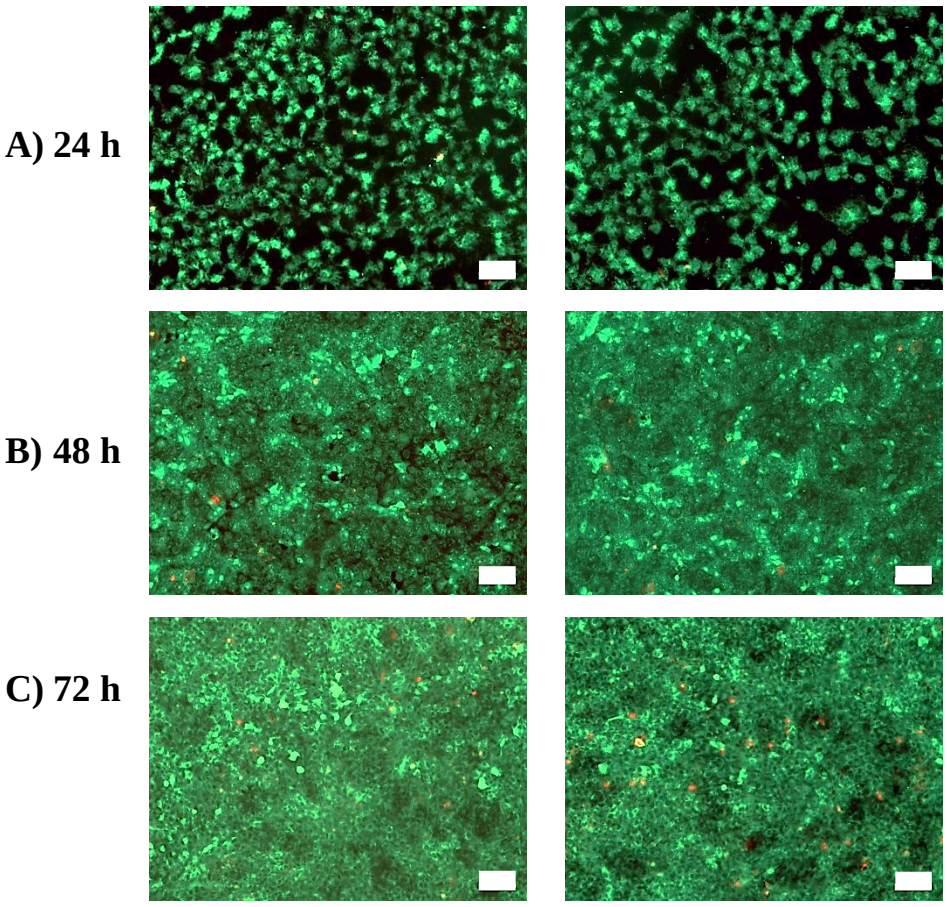

Fig. 4. *Representative pictures of Vero cell mat after A) 24 hours, B) 48 hours and C) 72 hours of polarization at 400 mV/SPR. Reactors seeded with 100 000 Vero cells; the potential of 400 mV/SPR was applied from the beginning; epifluorescent imaging after staining with Syto® and propidium iodine; scale bar 100 µm.*

Similar experiments were performed with Raw 264.7 cells, once again by applying the potential immediately after seeding the reactors. Six reactors were run in parallel, each seeded with 15 000

Raw 264.7 cells. Three values of the potential were used: -200, 0 and 400 mV/SPR, each on two reactors. Potentials were applied for 89 hours. After about half of the incubation time, the medium was replaced by fresh medium, great care being taken to avoid disturbing the cell mat.

The current records (Figure 5) were similar to those obtained with the Vero cells, with fairly stable values. As previously, low reduction currents were recorded at 200 mV/SPR, due to oxygen reduction. These reduction currents decreased slowly from about 400 to 200 nA. Residual currents were reductive at 0 mV/SPR, with a stable value of about 10 nA, and oxidative at 400 mV/SPR, stable around 20 nA.

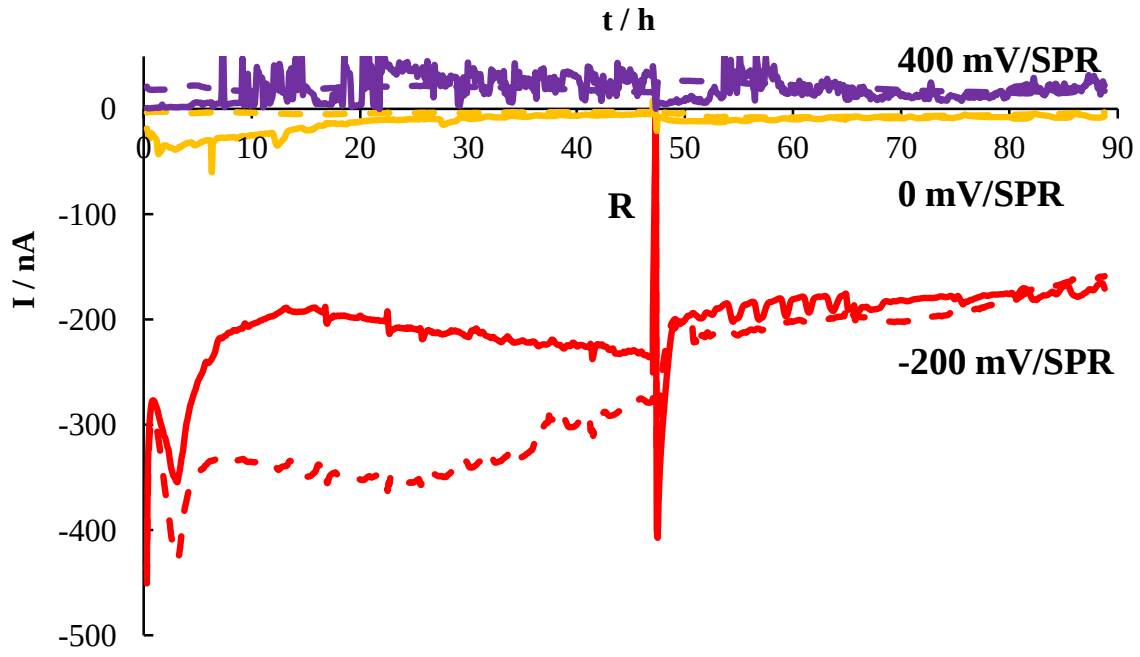

Fig. 5. *Current records when the potential was applied from the beginning. Red lines -200 mV/SPR, yellow lines 0 mV/SPR, purple lines 400 mV/SPR; reactors seeded with 15 000 Raw* 264.7 *cells; red lines: "R" at 47 hours indicates renewal of the medium; continuous and dotted lines are duplicates.*

Imaging at the end of the experiment confirmed the observations made with the Vero cells. There were hardly any cells adhering to the electrode exposed to the potentials of -200 and 0 mV/SPR, while the electrodes exposed to 400 mV/SPR displayed a dense mat of viable cells (Figures 6 and 7).

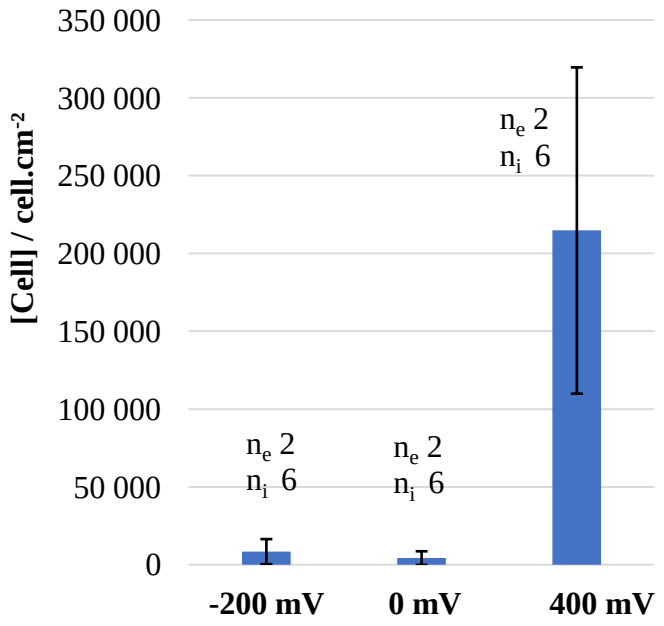

Fig. 6. *Number of adhered Raw* 264.7 *cells after 84 hours of incubation under applied potential of -200, 0 and 400 mV/SPR. Reactors seeded with 15 000 Raw* 264.7 *cells; potential was applied from the beginning.*

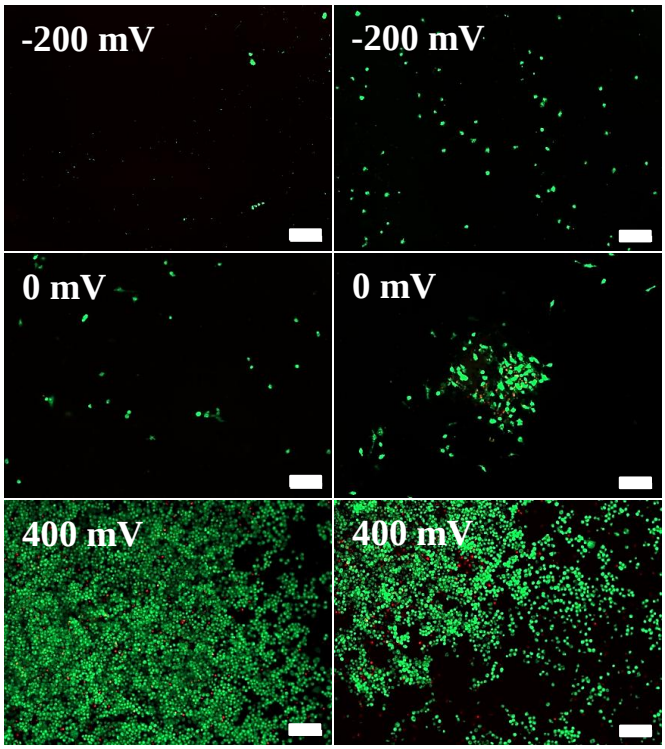

Fig. 7. *Representative pictures of the cell mats after 84 hours at (from top to bottom) -200, 0 and 400 mV/SPR. Reactors seeded with 15 000 Raw* 264.7 *cells; potential was applied from the beginning; epifluorescent imaging after staining with Syto9 ® and propidium iodide; scale bar 100 µm.*

Seeding with 15 000 cells can lead to a surface density of sedimented cells of 9 750 cell/cm^2. The cell density of 214 850 cell/cm^2 measured after 84 hours of polarization at 400 mV/SPR corresponded to more than 4 generations. It is consistent with the known doubling-time of 11-12 hours [49], which would allow 7 generations in 84 hours. Considering the compactness of the cell mat obtained at 400 mV/SPR, it can be assumed that cell development was slowed down by the densification of the mat or that the cells of the last generations were less firmly adhered to the mat and were removed during the sample preparation steps.

All the experiments confirm that the potentials of -200, 0 and 200 mV/SPR are deleterious for cell adhesion and proliferation. None of the 10 electrodes exposed to these different potential values, run in independent reactors, with two different cell lineages, exhibited cell colonization.

Moreover, applying these potential values after 24 hours of incubation performed without applied potential resulted in the release of cells previously adhered to the surface.

When the potential of -200 mV/SPR was applied, a reduction current was recorded, which was due to the reduction of dissolved oxygen [47]. This reaction can produce reactive oxygen species (ROS), for instance hydrogen peroxide by two-electron reduction of oxygen, particularly on carbon-based electrodes [50]. The deleterious effect of the potential of -200 mV/SPR on electrode colonization may consequently be attributed to the production of ROS, as already observed for metallic biomaterials [51,52].

The production of ROS could hardly be evoked for the 0 mV/SPR potential, at which the residual current was very low. It can definitively no longer be considered for 200 mV/SPR, at which the residual current was related to an oxidation reaction.

The residual current was in the reduction direction at 0 mV, while it was in the oxidation direction at 200 mV. So we cannot look for an explanation for the effect of the potential in the reduction/oxidation direction of the residual current.

To sum up, clear difference in the adhesion status was observed between the 10 independent electrodes run at the potentials of -200, 0 and 200 mV/SPR, which prohibited cell adhesion, versus the 10 independent electrodes run at 400 mV/SPR, which allowed surface colonization and cell proliferation. At the potentials of 0 and 200 mV/SPR, neither the possible production of ROS nor the reduction or oxidation status of the residual current can explain the repellent effect of the electrode surface regarding cell adhesion.

Cells adhered to the surface of the electrodes were viable after several days of polarization. Moreover, the potential of 400 mV/SPR seems to promote the production of thick cell mats, with a biofilm-like structure (Figure 3.C), which was never obtained by incubation of the same

duration without the applied potential (Figure 3.D). Nevertheless, such a modification of the cell mat structure was observed on most but not all the 10 electrodes that were polarized at 400 mV/SPR. Further work in this direction is needed to confirm the effect of the potential on the cell mat structure.

In order to progress in understanding the cause of the drastic switch of cell behaviour between the two potential ranges, abiotic experiments were performed to determine the potential of zero charge (pzc) of the electrode/solution interface. The charge of an electrode is negative when its potential is lower than the pzc and positive for potentials above the pzc. Cell adhesion is a process that is sensitive to the surface charge of the supporting material [10,12,28], so it seemed relevant to address the surface charge of the electrode.

The pzc of an electrode/solution interface can be assessed by using electrochemical impedance spectroscopy (EIS) to determine the value of the interfacial capacitance (C) as a function of the applied potential (E). The curve of C vs. E passes through a minimum, which corresponds to the pzc value [53,54]. As the pzc value depends on the material surface and on solution composition, measurements were made here in the same medium as that used for cell incubation and after having pre-treated the electrode following the same protocol as for cell incubation.

Here, the capacitance of the interface was determined by the Mott-Schottky method, which gives the value of the capacitance vs applied potential directly. In comparison to common EIS methods, Mott-Schottky allows faster measurements (although they did take a few hours) and thus avoids having too much change in the interface during, or because of, the measurement.

Mott-Schottky data are exploited at a fixed value of frequency. Here, the frequency was chosen on the basis of the Bode representation of experimental data (Figure 8.A). The Bode diagram had two sections: one section for frequencies above about 100 Hz, which was flat and corresponded to the purely resistive behaviour of the interface, and another section for frequency values below 100 Hz, which corresponded to the frequency range for which the interface behaviour was affected by its capacitive component. The value of 1 Hz, which was close to the middle of this section of the diagram, was chosen to extract the capacitances from the Mott-Schottky data. It was checked that fixing the frequency value at 100 mHz or 10 Hz led to similar conclusions.

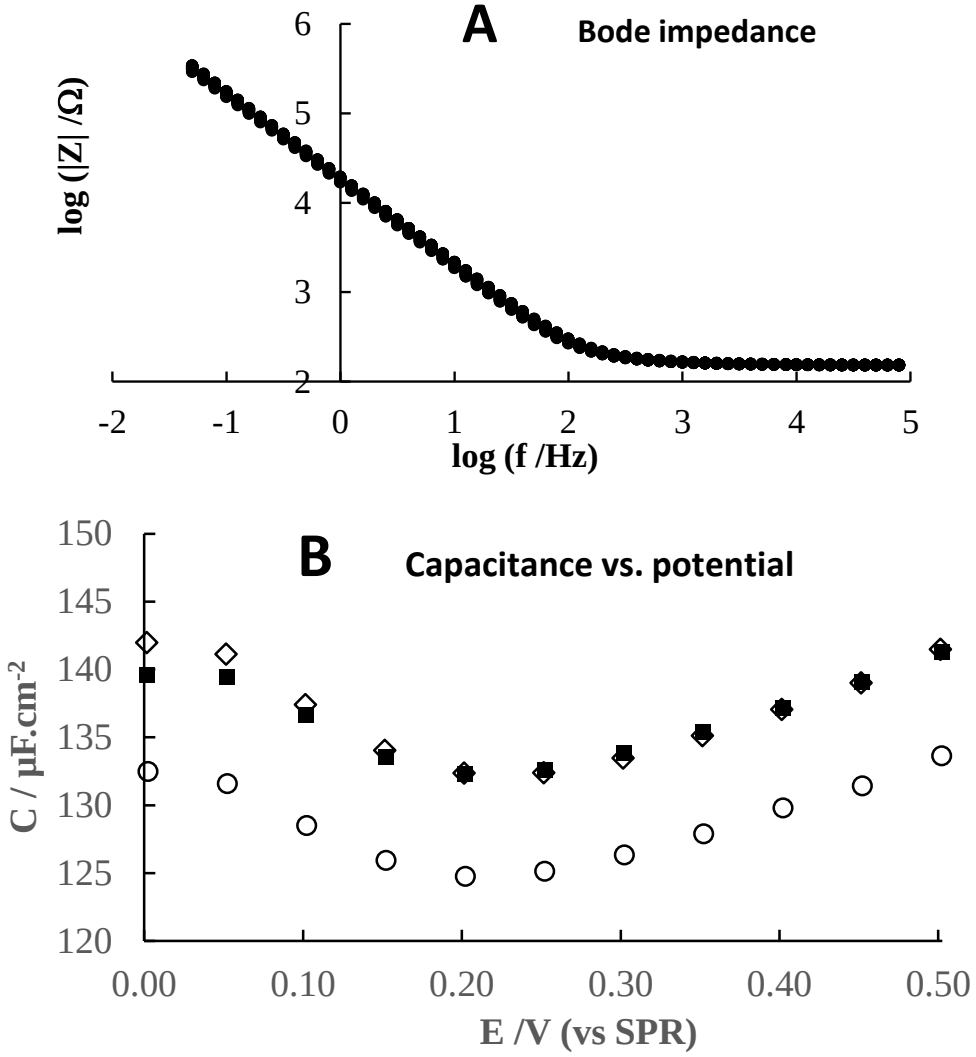

Fig. 8. *Measurement of the capacitance as a function of the applied potential by EIS. A) Bode representation of the logarithm of the impedance absolute value (|Z|) as a function of the logarithm of the frequency (f); the data recorded at the different values of the applied potential are almost superimposed because of the scale of the diagram chosen to represent the complete shape of the Bode curves. B) Capacitance as a function of the applied potential extracted from the Mott-Schottky curves for the frequency of 1 Hz (3 different electrodes).*

Generally, Mott-Schottky results are plotted in the form of $1/C^2$ vs. E, mainly to gain access to the number of charge carriers in the context of studies of semi-conductive materials [55]. Here, it is presented in the simple form of C vs. E (Figure 8.B). The potential range was restricted to between 0 and 400 mV/SPR because the occurrence of the reduction of oxygen at potentials below 0 mV/SPR disturbed the measurements. An electrical model including the oxygen

reduction reaction should be used to address the zone of lower potentials, rather than the simple model implemented by the Mott-Schottky method.

The value of the minimum of the C vs. E curve, extracted from 6 different electrodes, was 183 ± 20 mV/SPR for the first measurements, and it increased to 212 ± 31 mV/SPR for the second measurements. The 12 measurements on 6 different electrodes thus gave 198 ± 29 mV/SPR. Clearly, the pzc of the electrodes in the culture medium was located around 200 mV/SPR.

The change of the surface charge, from negative below around 200 mV to positive above, can explain the drastically different behaviour of the cells observed for -200, 0 and 200 mV/SPR on the one hand and 400 mV/SPR on the other hand.

The surface charge of the supporting material is a key parameter that is well known to affect cell adhesion and proliferation [56] and could also impact cell signalling processes that regulate cell differentiation [12]. Intuitively, a positive surface charge should promote the adhesion of cells by electrostatic interaction [57] if cells are assimilated to colloids with a globally negative external charge. However, the cell adhesion process is not so simple, because the proteins from the medium that are adsorbed on the electrode surface and those released by the cells play crucial roles in the mechanisms of cell adhesion and anchoring. Moreover, cells are far from being equivalent to inert colloidal species.

The molecular mechanisms of surface charge-dependent cellular activities still remain poorly understood, and both negatively and positively charged surfaces have been claimed to enhance cell adhesion [58]. Nevertheless, it has often been observed [10] or speculated [28] that positively charged surfaces promote cell adhesion, for instance by enhancing protein adsorption [12].

Here, both Vero and Raw 264.7 cells displayed the same drastic behaviour switch according to the value of the applied potential. The switch between no adhesion and adhesion occurred around the zero charge potential, so it is highly probable that the effect of potential was due to the surface charge of the electrode. At potentials of -200, 0 and 200 mV/SPR, the negative surface charge prevented cell adhesion while, at 400 mV/SPR, the positive charge allowed adhesion and proliferation.

The reason why the conclusion regarding the growth or non-growth of the cells depending on the value of the applied potential is so clear-cut, is probably that maintaining the potential imposed on the cells required a stable surface state of the support. Actually, in the absence of applied potential, the open-circuit potential of the support, its surface charge and other surface properties can be drastically modified by the cells. For instance, cells can change their ionic environment by ion exchanges through their plasma membrane. In the absence of applied potential, the effect of the redox status and the charge surface of the support can be compensated by the cells, which are able to create local conditions more favourable for their growth. The initial redox state and surface charge of the support should thus mainly affect the beginning of cell growth and their effect may then vanish upon the action of cells. In contrast, polarized supports maintain a stable redox status, which can be detrimental to cell development or, on the contrary, enhance it, during

the entire growth process. This leads to two types of conclusions. On the one hand, the results described here may be different from conclusions that could be extracted from works performed with non-polarized supports. On the other hand, one can think that the controlled-potential protocol offers an additional mode of action to guide cell development, which is different from simply choosing materials with given initial surface properties. This strategy has been little studied so far and the results obtained here show that it definitely deserves to be considered with more interest.

Conclusion

It is agreed that the electrochemical potential of the supporting surface is a crucial parameter for cell adhesion and proliferation. To date, the effects of the surface potential have been studied by comparing different materials or by changing the chemical composition of the surface coating to modify its potential. The difficulty in clearly separating the direct effect of the potential from that of the chemical composition of the material could thus be one of the reasons for the lack of clarity in this matter.

Here, the potential of the supporting surface was controlled by using a 3-electrode set-up, which allowed different potential values to be imposed on the same surface. The lowest potential values (up to 490 mv/SHE) inhibited cell adhesion and even detached cells that had previously adhered to the electrode surface. In contrast, the highest potential (690 mv/SHE) allowed effective cell adhesion and proliferation, in many cases even enhancing cell proliferation. These opposite behaviours correspond to values of potential below and above the zero charge potential (around 490 mV/SHE) and can therefore be related to the negative and positive charge of the electrode surface. Beyond the intrinsic interest of these results, this work confirms the interest of using 3-electrode set-ups to perform cell culture and tissue engineering in potential-controlled condition.

Acknowledgements

This work is part of the TECH project: “Looking for extracellular electron transfers with human cells” funded by the French Agence Nationale de la Recherche Scientifique (ANR-17-CE07-45). The authors thank Haouaria Belkhefa (Fonderephar) for helpful advice on cell cultures, L. Etchevery (Laboratoire de Génie Chimique) for help with electrochemical set-ups, and Dr Leila Haddioui (Fonderephar) for providing cells.

References

[1] K. Hosoyama, M. Ahumada, K. Goel, M. Ruel, E.J. Suuronen, E.I. Alarcon, Electroconductive materials as biomimetic platforms for tissue regeneration, Biotechnology Advances. 37 (2019) 444–458. https://doi.org/10.1016/j.biotechadv.2019.02.011.

[2] C. Ning, Z. Zhou, G. Tan, Y. Zhu, C. Mao, Electroactive polymers for tissue regeneration: Developments and perspectives, Progress in Polymer Science. 81 (2018) 144–162. https://doi.org/10.1016/j.progpolymsci.2018.01.001.

[3] R. Dong, P.X. Ma, B. Guo, Conductive biomaterials for muscle tissue engineering, Biomaterials. 229 (2020) 119584. https://doi.org/10.1016/j.biomaterials.2019.119584.

[4] S. Bechara, L. Wadman, K.C. Popat, Electroconductive polymeric nanowire templates facilitates in vitro C17.2 neural stem cell line adhesion, proliferation and differentiation, Acta Biomaterialia. 7 (2011) 2892–2901. https://doi.org/10.1016/j.actbio.2011.04.009.

[5] A. Orza, O. Soritau, L. Olenic, M. Diudea, A. Florea, D. Rus Ciuca, C. Mihu, D. Casciano, A.S. Biris, Electrically Conductive Gold-Coated Collagen Nanofibers for Placental-Derived Mesenchymal Stem Cells Enhanced Differentiation and Proliferation, ACS Nano. 5 (2011) 4490–4503. https://doi.org/10.1021/nn1035312.

[6] T.-H. Kim, W.A. El-Said, J.H. An, J.-W. Choi, ITO/gold nanoparticle/RGD peptide composites to enhance electrochemical signals and proliferation of human neural stem cells, Nanomedicine: Nanotechnology, Biology and Medicine. 9 (2013) 336–344. https://doi.org/10.1016/j.nano.2012.08.006.

[7] G. Jin, K. Li, The electrically conductive scaffold as the skeleton of stem cell niche in regenerative medicine, Materials Science and Engineering: C. 45 (2014) 671–681. https://doi.org/10.1016/j.msec.2014.06.004.

[8] S. Aznar-Cervantes, J.G. Martínez, A. Bernabeu-Esclapez, A.A. Lozano-Pérez, L. Meseguer-Olmo, T.F. Otero, J.L. Cenis, Fabrication of electrospun silk fibroin scaffolds coated with graphene oxide and reduced graphene for applications in biomedicine, Bioelectrochemistry. 108 (2016) 36–45. https://doi.org/10.1016/j.bioelechem.2015.12.003.

[9] G. Cellot, E. Cilia, S. Cipollone, V. Rancic, A. Sucapane, S. Giordani, L. Gambazzi, H. Markram, M. Grandolfo, D. Scaini, F. Gelain, L. Casalis, M. Prato, M. Giugliano, L. Ballerini, Carbon nanotubes might improve neuronal performance by favouring electrical shortcuts, Nature Nanotech. 4 (2009) 126–133. https://doi.org/10.1038/nnano.2008.374.

[10] H.-Y. Chang, W.-L. Kao, Y.-W. You, Y.-H. Chu, K.-J. Chu, P.-J. Chen, C.-Y. Wu, Y.-H. Lee, J.-J. Shyue, Effect of surface potential on epithelial cell adhesion, proliferation and morphology,

Colloids and Surfaces B: Biointerfaces. 141 (2016) 179–186. https://doi.org/10.1016/j.colsurfb.2016.01.049.

[11] A.M. Ross, Z. Jiang, M. Bastmeyer, J. Lahann, Physical aspects of cell culture substrates: topography, roughness, and elasticity, Small. 8 (2012) 336–355. https://doi.org/10.1002/smll.201100934.

[12] S. Metwally, U. Stachewicz, Surface potential and charges impact on cell responses on biomaterials interfaces for medical applications, Mater Sci Eng C Mater Biol Appl. 104 (2019) 109883. https://doi.org/10.1016/j.msec.2019.109883.

[13] J.H. Lee, H.W. Jung, I.-K. Kang, H.B. Lee, Cell behaviour on polymer surfaces with different functional groups, Biomaterials. 15 (1994) 705–711. https://doi.org/10.1016/0142-9612(94)90169-4.

[14] T.G. van Kooten, J.M. Schakenraad, H.C. van der Mei, H.J. Busscher, Influence of substratum wettability on the strength of adhesion of human fibroblasts, Biomaterials. 13 (1992) 897–904. https://doi.org/10.1016/0142-9612(92)90112-2.

[15] K. Nakazawa, Y. Izumi, R. Mori, Morphological and functional studies of rat hepatocytes on a hydrophobic or hydrophilic polydimethylsiloxane surface, Acta Biomater. 5 (2009) 613–620. https://doi.org/10.1016/j.actbio.2008.08.011.

[16] M. Nikkhah, F. Edalat, S. Manoucheri, A. Khademhosseini, Engineering microscale topographies to control the cell–substrate interface, Biomaterials. 33 (2012) 5230–5246. https://doi.org/10.1016/j.biomaterials.2012.03.079.

[17] L. Tian, M.P. Prabhakaran, J. Hu, M. Chen, F. Besenbacher, S. Ramakrishna, Synergistic effect of topography, surface chemistry and conductivity of the electrospun nanofibrous scaffold on cellular response of PC12 cells, Colloids and Surfaces B: Biointerfaces. 145 (2016) 420–429. https://doi.org/10.1016/j.colsurfb.2016.05.032.

[18] R. Balint, N.J. Cassidy, S.H. Cartmell, Conductive polymers: Towards a smart biomaterial for tissue engineering, Acta Biomaterialia. 10 (2014) 2341–2353. https://doi.org/10.1016/j.actbio.2014.02.015.

[19] C. Gardin, A. Piattelli, B. Zavan, Graphene in Regenerative Medicine: Focus on Stem Cells and Neuronal Differentiation, Trends in Biotechnology. 34 (2016) 435–437. https://doi.org/10.1016/j.tibtech.2016.01.006.

[20] S.-Y. Wu, S.S.A. An, J. Hulme, Current applications of graphene oxide in nanomedicine, Int J Nanomedicine. 10 (2015) 9–24. https://doi.org/10.2147/IJN.S88285.

[21] M. Rimboud, D. Pocaznoi, B. Erable, A. Bergel, Electroanalysis of microbial anodes for bioelectrochemical systems: basics, progress and perspectives, Phys. Chem. Chem. Phys. 16 (2014) 16349–16366. https://doi.org/10.1039/c4cp01698j.

[22] S.F. Ketep, A. Bergel, M. Bertrand, W. Achouak, E. Fourest, Lowering the applied potential during successive scratching/re-inoculation improves the performance of microbial anodes for microbial fuel cells, Bioresource Technology. 127 (2013) 448–455. https://doi.org/10.1016/j.biortech.2012.09.008.

[23] R. Rousseau, C. Santaella, A. Bonnafous, W. Achouak, J.-J. Godon, M.-L. Delia, A. Bergel, Halotolerant bioanodes: The applied potential modulates the electrochemical characteristics, the biofilm structure and the ratio of the two dominant genera, Bioelectrochemistry. 112 (2016) 24–32. https://doi.org/10.1016/j.bioelechem.2016.06.006.

[24] D.-B. Li, J. Li, D.-F. Liu, X. Ma, L. Cheng, W.-W. Li, C. Qian, Y. Mu, H.-Q. Yu, Potential regulates metabolism and extracellular respiration of electroactive Geobacter biofilm, Biotechnology and Bioengineering. 0 (2019). https://doi.org/10.1002/bit.26928.

[25] F. Scarabotti, L. Rago, K. Bühler, F. Harnisch, The electrode potential determines the yield coefficients of early-stage Geobacter sulfurreducens biofilm anodes, Bioelectrochemistry. 140 (2021) 107752. https://doi.org/10.1016/j.bioelechem.2021.107752.

[26] S. Guette-Marquet, C. Roques, A. Bergel, Theoretical analysis of the electrochemical systems used for the application of direct current/voltage stimuli on cell cultures, Bioelectrochemistry. 139 (2021) 107737. https://doi.org/10.1016/j.bioelechem.2020.107737.

[27] Q. Qiu, M. Sayer, X. Shen, J.E. Davies, A system designed for the study of cell activity under electrical stimulation, Biotechnol Tech. 9 (1995) 209–214. https://doi.org/10.1007/BF00157080.

[28] Q. Qiu, M. Sayer, M. Kawaja, X. Shen, J.E. Davies, Attachment, morphology, and protein expression of rat marrow stromal cells cultured on charged substrate surfaces, Journal of Biomedical Materials Research. 42 (1998) 117–127. https://doi.org/10.1002/(SICI)1097-4636(199810)42:1<117::AID-JBM15>3.0.CO;2-I.

[29] P.N. Sawyer, W.H. Brattain, P.J. Boddy, Electrochemical Precipitation of Human Blood Cells and Its Possible Relation to Intravascular Thrombosis, PNAS. 51 (1964) 428–432. https://doi.org/10.1073/pnas.51.3.428.

[30] H. Shinohara, J. Kojima, M. Yaoita, M. Aizawa, Electrically stimulated rupture of cell membranes with a conducting polymer-coated electrode, Bioelectrochemistry and Bioenergetics. 22 (1989) 23–35. https://doi.org/10.1016/0302-4598(89)85027-5.

[31] M.M. Goldin, A.G. Volkov, Y.S. Goldfarb, M.M. Goldin, Electrochemical Aspects of Hemosorption, J. Electrochem. Soc. 153 (2006) J91. https://doi.org/10.1149/1.2208910.

[32] A.N. Kuzovlev, A.K. Evseev, I.V. Goroncharovskaya, A.K. Shabanov, S.S. Petrikov, Optically transparent electrodes to study living cells: A mini review, Biotechnology and Bioengineering. 118 (2021) 2393–2400. https://doi.org/10.1002/bit.27782.

[33] J.Y. Wong, R. Langer, D.E. Ingber, Electrically conducting polymers can noninvasively control the shape and growth of mammalian cells., PNAS. 91 (1994) 3201–3204. https://doi.org/10.1073/pnas.91.8.3201.

[34] J. Kojima, H. Shinohara, Y. Ikariyama, M. Aizawa, K. Nagaike, S. Morioka, Electrically promoted protein production by mammalian cells cultured on the electrode surface, Biotechnology and Bioengineering. 39 (1992) 27–32. https://doi.org/10.1002/bit.260390106.

[35] J. Feng, G.-A. Luo, H.-Y. Jian, R.-G. Wang, C.-C. An, Voltammetric Behavior of Tumor Cells U937 and Its Usefulness in Evaluating the Effect of Caffeic Acid, Electroanalysis. 12 (2000) 513–516. https://doi.org/10.1002/(SICI)1521-4109(200005)12:7<513::AID-ELAN513>3.0.CO;2-D.

[36] D.-M. Wu, G.-L. Fu, H.-Z. Fang, L. Hu, J.-L. Li, X. Yuan, Z.-Y. Zhang, Studies on the origin of the voltammetric response of the PC-3 cell suspension, Talanta. 78 (2009) 602–607. https://doi.org/10.1016/j.talanta.2008.12.016.

[37] W.A. El-Said, C.-H. Yea, H. Kim, B.-K. Oh, J.-W. Choi, Cell-based chip for the detection of anticancer effect on HeLa cells using cyclic voltammetry, Biosensors and Bioelectronics. 24 (2009) 1259–1265. https://doi.org/10.1016/j.bios.2008.07.037.

[38] W.A. El-Said, T.-H. Kim, H. Kim, J.-W. Choi, Detection of effect of chemotherapeutic agents to cancer cells on gold nanoflower patterned substrate using surface-enhanced Raman scattering and cyclic voltammetry, Biosensors and Bioelectronics. 26 (2010) 1486–1492. https://doi.org/10.1016/j.bios.2010.07.089.

[39] C.-H. Yea, H.-C. Jeong, S.-H. Moon, M.-O. Lee, K.-J. Kim, J.-W. Choi, H.-J. Cha, In situ label-free quantification of human pluripotent stem cells with electrochemical potential, Biomaterials. 75 (2016) 250–259. https://doi.org/10.1016/j.biomaterials.2015.10.038.

[40] M. Haeri, T. Wöllert, G.M. Langford, J.L. Gilbert, Voltage-controlled cellular viability of preosteoblasts on polarized cpTi with varying surface oxide thickness, Bioelectrochemistry. 94 (2013) 53–60. https://doi.org/10.1016/j.bioelechem.2013.06.002.

[41] J.L. Gilbert, L. Zarka, E. Chang, C.H. Thomas, The reduction half cell in biomaterials corrosion: Oxygen diffusion profiles near and cell response to polarized titanium surfaces, Journal of Biomedical Materials Research. 42 (1998) 321–330. https://doi.org/10.1002/(SICI)1097-4636(199811)42:2<321::AID-JBM18>3.0.CO;2-L.

[42] M. Haeri, T. Wöllert, G.M. Langford, J.L. Gilbert, Electrochemical control of cell death by reduction-induced intrinsic apoptosis and oxidation-induced necrosis on CoCrMo alloy in vitro, Biomaterials. 33 (2012) 6295–6304. https://doi.org/10.1016/j.biomaterials.2012.05.054.

[43] J.S. Rhim, K. Schell, B. Creasy, W. Case, Biological Characteristics and Viral Susceptibility of an African Green Monkey Kidney Cell Line (Vero), Proceedings of the Society for Experimental Biology and Medicine. 132 (1969) 670–678. https://doi.org/10.3181/00379727-132-34285.

[44] P.N. Barrett, S.J. Terpening, D. Snow, R.R. Cobb, O. Kistner, Vero cell technology for rapid development of inactivated whole virus vaccines for emerging viral diseases, Expert Review of Vaccines. 16 (2017) 883–894. https://doi.org/10.1080/14760584.2017.1357471.

[45] F. Aubrit, F. Perugi, A. Léon, F. Guéhenneux, P. Champion-Arnaud, M. Lahmar, K. Schwamborn, Cell substrates for the production of viral vaccines, Vaccine. 33 (2015) 5905–5912. https://doi.org/10.1016/j.vaccine.2015.06.110.

[46] C.A. Schneider, W.S. Rasband, K.W. Eliceiri, NIH Image to ImageJ: 25 years of image analysis, Nat Methods. 9 (2012) 671–675. https://doi.org/10.1038/nmeth.2089.

[47] S. Guette-Marquet, C. Roques, A. Bergel, Catalysis of the electrochemical oxygen reduction reaction (ORR) by animal and human cells, PLOS ONE. 16 (2021) e0251273. https://doi.org/10.1371/journal.pone.0251273.

[48] A.T. Nahapetian, J.N. Thomas, W.G. Thilly, Optimization of environment for high density Vero cell culture: effect of dissolved oxygen and nutrient supply on cell growth and changes in metabolites, Journal of Cell Science. 81 (1986) 65–103. https://doi.org/10.1242/jcs.81.1.65.

[49] I. Assanga, Cell growth curves for different cell lines and their relationship with biological activities, Int. J. Biotechnol. Mol. Biol. Res. 4 (2013) 60–70. https://doi.org/10.5897/IJBMBR2013.0154.

[50] M.E. Lai, A. Bergel, Electrochemical reduction of oxygen on glassy carbon: catalysis by catalase, Journal of Electroanalytical Chemistry. 494 (2000) 30–40. https://doi.org/10.1016/S0022-0728(00)00307-7.

[51] M. Haeri, J.L. Gilbert, Study of cellular dynamics on polarized CoCrMo alloy using time-lapse live-cell imaging, Acta Biomaterialia. 9 (2013) 9220–9228. https://doi.org/10.1016/j.actbio.2013.06.040.

[52] S. Sivan, S. Kaul, J.L. Gilbert, The effect of cathodic electrochemical potential of Ti-6Al-4V on cell viability: voltage threshold and time dependence, Journal of Biomedical Materials Research Part B: Applied Biomaterials. 101 (2013) 1489–1497. https://doi.org/10.1002/jbm.b.32970.

[53] A. Łukomska, J. Sobkowski, Potential of zero charge of monocrystalline copper electrodes in perchlorate solutions, Journal of Electroanalytical Chemistry. 567 (2004) 95–102. https://doi.org/10.1016/j.jelechem.2003.11.063.

[54] M.A. Amin, S.S. Abd El-Rehim, E.E.F. El-Sherbini, R.S. Bayoumi, The inhibition of low carbon steel corrosion in hydrochloric acid solutions by succinic acid: Part I. Weight loss, polarization, EIS, PZC, EDX and SEM studies, Electrochimica Acta. 52 (2007) 3588–3600. https://doi.org/10.1016/j.electacta.2006.10.019.

[55] L. Pons, M.-L. Délia, R. Basséguy, A. Bergel, Effect of the semi-conductive properties of the passive layer on the current provided by stainless steel microbial cathodes, Electrochimica Acta. 56 (2011) 2682–2688. https://doi.org/10.1016/j.electacta.2010.12.039.

[56] H.-Y. Chang, C.-C. Huang, K.-Y. Lin, W.-L. Kao, H.-Y. Liao, Y.-W. You, J.-H. Lin, Y.-T. Kuo, D.-Y. Kuo, J.-J. Shyue, Effect of Surface Potential on NIH3T3 Cell Adhesion and Proliferation, J. Phys. Chem. C. 118 (2014) 14464–14470. https://doi.org/10.1021/jp504662c.

[57] A.S.G. Curtis, THE MECHANISM OF ADHESION OF CELLS TO GLASS, J Cell Biol. 20 (1964) 199–215.

[58] H.-I. Chang, Y. Wang, Cell Responses to Surface and Architecture of Tissue Engineering Scaffolds | IntechOpen, Regen. Med. Tissue Eng. - Cells Biomater. (2011). https://www.intechopen.com/chapters/19013 (accessed September 6, 2021).